

A Theoretical and Experimental Study
of Concrete Beams - Especially Over-
Reinforced Beams - Subjected to Torsion
Part I. Theory

John Sander Nielsen

Serie R

No 170

1983

A THEORETICAL AND EXPERIMENTAL
STUDY OF CONCRETE BEAMS
- ESPECIALLY OVER-REINFORCED BEAMS -
SUBJECTED TO TORSION

PART I
THEORY

JOHN SANDER NIELSEN

AFDELINGEN FOR BÆRENDE KONSTRUKTIONER, DANMARKS TEKNISKE HØJSKOLE
DEPARTMENT OF STRUCTURAL ENGINEERING, TECHNICAL UNIVERSITY OF DENMARK

Preface

This report has been prepared as part of the conditions for acquiring the Danish Ph.D. degree in structural engineering.

The study has been carried out at the Department of Structural Engineering, Technical University of Denmark under the guidance of Professor, dr.techn. Troels Brøndum-Nielsen. M.W. Bråstrup and E. Skettrup have acted as consultants.

Lyngby, September 1983.

John Sander Nielsen

<u>Contents</u>	Page
Notation	3
Summary	4
Summary in Danish (Dansk Resumé)	5
1. Introduction	6
2. Model proposed by D. Mitchell and M.P. Collin	7
3. Test observations	8
3.1 Dependence of carrying capacity on arrangement of reinforcement	12
3.2 Dependence of carrying capacity on depth of concrete cover	12
3.3 Rupture pattern	12
4. Theoretical Solution	20
4.1 Lower bound solution	21
4.2 Determination of maximum concrete compression , n_{by}	27
4.2.1 Determination of n_{vby} on the basis of the theory of plasticity	29
4.2.1.1 Description of rupture pattern	32
5. Comparison with tests	35
6. Conclusions and discussion	41
References	48

NOTATION

- T = Torsional moment
- n_1 = The force in the reinforcement per unit length
(in the stirrup direction)
- n_{1y} = n_1 at yield in the reinforcement
- n_s = The force in the reinforcement per unit length
(in the longitudinal direction)
- n_{sy} = n_s at yield in the reinforcement
- n_b = The compression force in the concrete per unit
length (in the direction perpendicular to the
compression)
- n = The shear force per unit length of the rectangle
formed by the corner bars
- n_x = Normal force in the x-direction (per unit length)
- n_y = Normal force in the y-direction (per unit length)
- σ_c = The compression strength of the concrete
- σ_t = The split tensile strength of the concrete
- σ_f = The pressure per square unit just below the corner
bars
- σ_{Fl} = The yield stress in the longitudinal reinforcement
- σ_{Fb} = The yield stress in the stirrup reinforcement
- v_c = Efficiency factor for concrete compression strength
- v_t = Efficiency factor for tensile strength in the concrete
- $\left. \begin{array}{l} a \\ b \end{array} \right\}$ = The side length of the rectangle formed by the longitudinal
reinforcement
- d = The diameter of the longitudinal reinforcing bar located
at the corner of the cross section
- S = Spacing of hoops
- \emptyset = Angle of diagonal compression
- φ = Angle of friction
- β = Half the apex of the wedge just below the corner bars

Summary

This thesis is not intended as a study of the literature on torsion in concrete structures. Lennart Elfgren and Inge Karlsson [1] published such a study in December 1969, and the American Concrete Institute is preparing a "bibliography on torsion".

I have therefore refrained from such a study, and my thesis contains at any rate partially original work except for section 2. This section describes the theory developed by Denis Mitchell and Michael P. Collins 2 : "The diagonal compression field theory", which deals with both normally reinforced and over-reinforced concrete beams subjected to pure torsion. The section in question has been included partly on account of the time of publication (later than 1969, viz. March 1974) and partly on account of the merit of the theory.

Section 3 contains a report on observations made regarding the mode of rupture of over-reinforced beams during a test series with concrete beams subjected to torsion performed at the Department of Structural Engineering of the Technical University of Denmark.

In section 4 I have made an attempt to find a method of calculating the carrying capacity of over-reinforced concrete beams. The method of analysis described is in accordance with the observations made during the test series reported in section 3.

Section 5 contains a comparison between tests and the theory established and section 6 contains conclusions.

Summary in Danish (Dansk Resumé)

Denne afhandling er ikke ment som en gennemgang af litteraturen omhandlende vridning i betonkonstruktioner. En sådan er foretaget af Lennart Elfgren og Inge Karlsson i december 1969 [1], og American Concrete Institute forbereder udsendelsen af en "bibliography on torsion".

Jeg har derfor afstået fra en sådan gennemgang, og afhandlingen indeholder af ikke - i hvert fald delvis - originalt arbejde kun afsnit 2. Dette afsnit beskriver den af Denis Mitchell og Michael P. Collins [2] udviklede teori "The Diagonal Compression Fields Theory", der omhandler såvel normalt armerede som overarmerede betonbjælker påvirket til ren vridning. Dette afsnit er medtaget dels på grund af publiceringstidspunktet (senere end 1969 - nemlig marts 1974), dels på grund af teoriens lødighed.

Afsnit 3 er en redegørelse for iagttagelser vedrørende brudmåden for overarmerede bjælker foretaget under en forsøgsserie med vridningspåvirkede betonbjælker udført på Afdelingen for Bærende Konstruktioner, Danmarks tekniske Højskole.

I afsnit 4 gøres et forsøg på at finde en beregningsmåde for bæreevnen af overarmerede betonbjælker - en beregningsmåde, der er i overensstemmelse med iagttagelserne gjort under forsøgsserien omtalt i afsnit 3.

Sammenligning mellem forsøg og den opstillede teori er foretaget i afsnit 5, medens afsnit 6 indeholder konklusioner.

1. Introduction

When studying the literature on reinforced concrete structures subjected to torsion, one is struck by the disproportion between the large number of research workers who concern themselves, or have concerned themselves, with normally reinforced structures, and the very small number who have paid attention to over-reinforced structures.

This can be defended in the case of structures subjected to pure torsion since here, in practice, it is enough to interest oneself in an upper limit for the quantity of reinforcement and consequently unnecessary to concern oneself with how the concrete resists the load.

For most of the structures in practice, the governing load is, however, a combination of two or more of the following moments and forces:

- Bending moment
- Torsional moment
- Shear force
- Normal force

In this case, in order to be able to combine the effects in the concrete, it is essential to know how each of the effects is resisted since it would otherwise be difficult to get an idea of how the combined effect is resisted (although this is not to say that one can use the superposition principle).

I have therefore carried out this work with a view to contributing to our understanding of how the load pure torsion is resisted in the concrete, and the case - combined effects - is only touched upon here and there in order to demonstrate the aim of the project.

Of studies that can be used as a basis for mapping the development of stresses in concrete structures exposed to combined effects, I will discuss that of Denis Mitchell and Michael P. Collins [2], although some of the assumptions made by these authors are at variance with the test material mentioned here [3].

2. Model of Denis Mitchell and Michael P. Collins [2].

The aim of these authors was to arrive at a model which, in simplicity and stringency, lay close to the models used for bending stresses.

The system of equations established consists of three main ingredients:

- 1: equilibrium equations
- 2: geometrical criteria
- 3: physical relations

- re. 1) A lattice analogy consideration is used, with variable slope of the compression in the concrete.
- re. 2) A geometrical relationship is established between strains in the steel, strains in the concrete and the angle of torsion of the beam. In addition, a relationship is established between the angle of torsion and the curvature of the concrete compression bars.
- re. 3) For the steel, the stress-strain curves achieved on the basis of tests are used, while the compressive stress-strain curve for the concrete is a parabola, and its tensile strength is put at 0.

The resulting system of equations, combined with a number of assumptions, constitutes a system that is sufficient to allow computation of both stress-strain curve and rupture load for a given part of a structure. The assumptions include the following:

- a) that the concrete lying outside the centroid of the stirrup reinforcement does not participate in the force resistance.
- b) that the concrete pressure in the lattice analogy model assumes such a direction that the angle of rotation of the beam for a given torsional moment is minimized.
- c) that the concrete fails in compression when the strain in the outermost concrete layer exceeds 0.3%.

3. Test observations

In the autumn of 1975 and the spring of 1976 a series of tests on over-reinforced concrete beams subjected to pure torsion was carried out at the Structural Research Laboratory.

The tests were carried out by John Sander Nielsen and Professor dr.techn. Troels Brøndum-Nielsen.

The purpose of the tests was as follows:

- 1: to investigate the effect of the arrangement of the reinforcement on the carrying capacity
- 2: to clarify the dependence of the ultimate carrying capacity on the thickness of the concrete cover
- 3: to investigate the rupture pattern for over-reinforced cross sections.

Tables 1 to 3 show in brief form the most important data from the tests. For a detailed description of the beams used, the execution of the tests and the results, see [3].

TABEL 1.

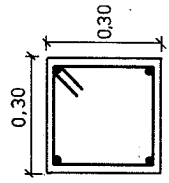
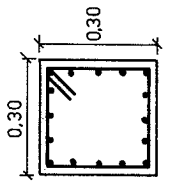
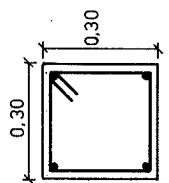
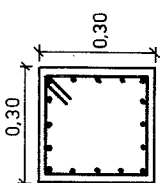
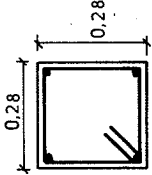
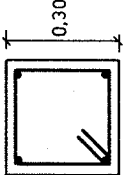
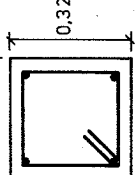
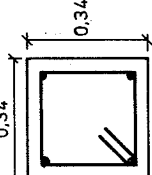
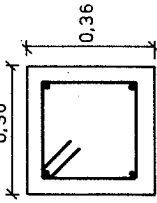
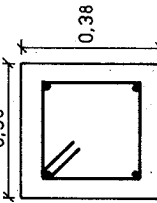
No.	Cross section m	Longitudinal reinforcement		Stirrup reinforcement		Concrete compression strength MPa	Measured rupture values KNm
		Quantity	Grade	Spacing, dimension mm	Grade		
I A1		4 ϕ 12	KS 42 S $\sigma_y \approx 420$ MPa	111, ϕ 8	KS 42 S $\sigma_y \approx 420$ MPa	29.08	29.32
I A2		16 ϕ 6	KS 42 S	101, ϕ 8	KS 42 S	29.55	26.40
I A3		16 ϕ 6	KS 42 S $\sigma_y \approx 420$ MPa		KS 42 S $\sigma_y \approx 420$ MPa	23.63	24.68
I B1		4 ϕ 12	KS 60 S $\sigma_y \approx 600$ MPa	111, ϕ 8	KS 60 S $\sigma_y \approx 600$ MPa	28.24	35.08
I B2		16 ϕ 6	KS 60 S	101, ϕ 8	KS 60 S	24.54	29.80
I B3		16 ϕ 6	KS 60 S $\sigma_y \approx 600$ MPa		KS 60 S $\sigma_y \approx 600$ MPa	25.39	30.28

TABLE 2.

No.	Cross section m	Longitudinal reinforcement		Stirrup reinforcement		Concrete compression strength MPa	Measured rupture values KNm
		Quantity	Grade	Spacing, dimension mm	Grade		
II-0		4 ϕ 12	KS 90 S	81, ϕ 8	KS 60 S	23.79	34.68
II-1		4 ϕ 12	KS 90 S $\sigma_y \approx 900$ MPa	81, ϕ 8	KS 60 S $\sigma_y \approx 600$ MPa	26.17	34.84
II-2		4 ϕ 12	KS 90 S	81, ϕ 8	KS 60 S	27.26	39.16
II-3		4 ϕ 12	KS 90 S $\sigma_y \approx 900$ MPa	81, ϕ 8	KS 60 S $\sigma_y \approx 600$ MPa	21.61	33.57
II-4		4 ϕ 12	KS 90 S	81, ϕ 8	KS 60 S	23.20	33.76
II-4*		4 ϕ 12	KS 90 S $\sigma_y \approx 900$ MPa	81, ϕ 8	KS 60 S $\sigma_y \approx 600$ MPa	23.53	35.36
II-5		4 ϕ 12	KS 90 S	81, ϕ 8	KS 60 S	22.68	34.04
II-5*		4 ϕ 12	KS 90 S $\sigma_y \approx 900$ MPa	81, ϕ 8	KS 60 S $\sigma_y \approx 600$ MPa	26.41	38.04

TABEL 3.

No.	Cross section m	Longitudinal reinforcement		Stirrup reinforcement		Concrete compression strength MPa	Measured rupture values KNm
		Quantity	Grade	Spacing, dimension mm	Grade		
II-6		4 \emptyset 12	KS 90 S	81, \emptyset 7	KS 60 S	25.10	33.54
II-6*		4 \emptyset 12	KS 90 S	81, \emptyset 7	KS 60 S	27.67	37.38
II-7		4 \emptyset 12	KS 90 S $\sigma_y \approx 900$ MPa	81, \emptyset 7	KS 60 S $\sigma_y \approx 600$ MPa	27.55	34.20
II-8		4 \emptyset 12	KS 90 S	81, \emptyset 7	KS 60 S	21.80	32.88
II-9		4 \emptyset 12	KS 90 S $\sigma_y \approx 900$ MPa	81, \emptyset 7	KS 60 S $\sigma_y \approx 600$ MPa	21.95	34.28

3.1 Dependence of carrying capacity on arrangement of the reinforcement.

A comparison of beams IB2 and IB3 with beams II-0 to II-9 shows clearly that the carrying capacity of the former was considerably lower than that of the latter even though none of the beams reached yielding in the reinforcement. The difference observed must therefore be attributed to differences in the construction of the reinforcement. The main difference here is that IB2 and IB3 had axial reinforcement of 6 mm deformed steel, while II-0 to II-9 had axial reinforcement consisting of 12 mm deformed steel. It must therefore be concluded that the design of the arrangement of the reinforcement affects the carrying capacity of over-reinforced concrete beams subjected to pure torsion.

3.2 Dependence of carrying capacity on depth of concrete cover.

It was not possible from the tests carried out to demonstrate any relationship between the depth of the concrete cover and the rupture load, and as the depths used in the tests must cover all cases occurring in practice, it can be concluded that the ultimate carrying capacity of over-reinforced concrete beams subjected to pure torsion is independent of the depth of the concrete cover.

3.3 Rupture pattern

The rupture pattern described in this section is based on observations taken during the 19 tests described in [3] on over-reinforced concrete beams subjected to torsion and the 12 torsional tests described in [4] on normally reinforced concrete beams.

At rupture, the interaction between the concrete and the reinforcement in over-reinforced beams was found to differ significantly from that in normally reinforced beams.

In the over-reinforced beams, the part of the concrete lying outside the rectangle formed by the axial reinforcement showed spalling, whereas this was not the case in the normally reinforced beams. This spalling must not be confused either with the spalling that occurs after rupture as consequence of continued application of angle of rotation or with possible spalling of the concrete corners of the cross section. Fig. 1 shows schematically how the spalling occurs, while fig. 2 shows a cross section of beam II-8, in which the spalling crack can be clearly seen.

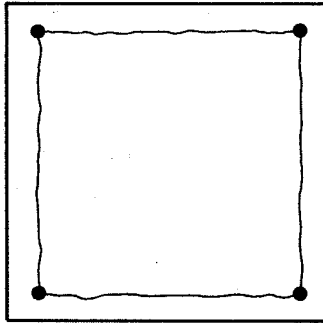


fig. 1.

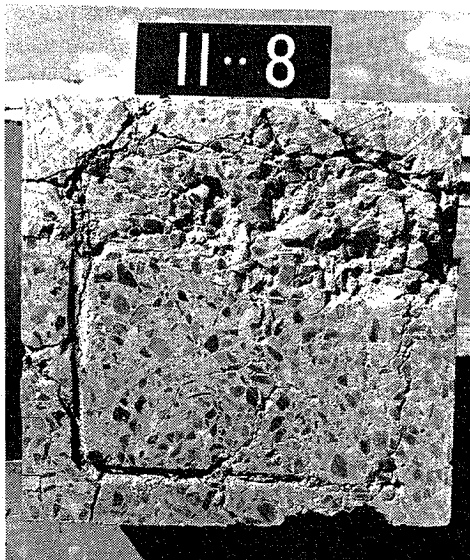


fig. 2.

In order to throw more light on the problem, we can consider beams IA3 and IB2 (see table 1). The concrete dimensions and the arrangement of the reinforcement are the same in the two beams, but the reinforcement in beam IA3 is Swedish deformed steel KS42S, while in beam IB2, it is KS60S (see Part II for detailed information on beams and materials).

Beam IA3 proved to be normally reinforced, while beam IB2 was over-reinforced.

After rupture, both beams were sawed through, and a clear difference could be seen in their crack pictures. The above-mentioned cracking connecting the longitudinal reinforcing bars can be seen in fig. 4, whereas there are no signs at all of it in fig. 3.

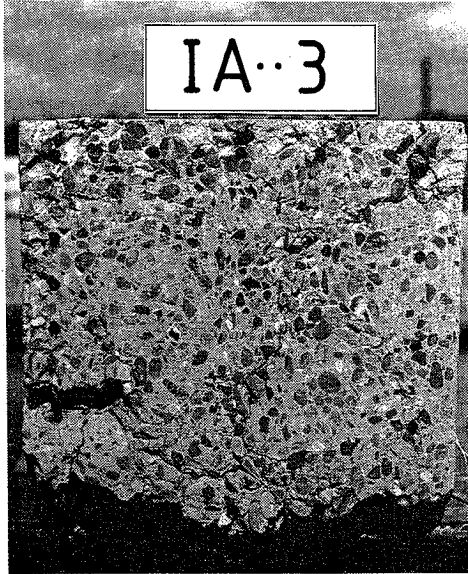


fig. 3

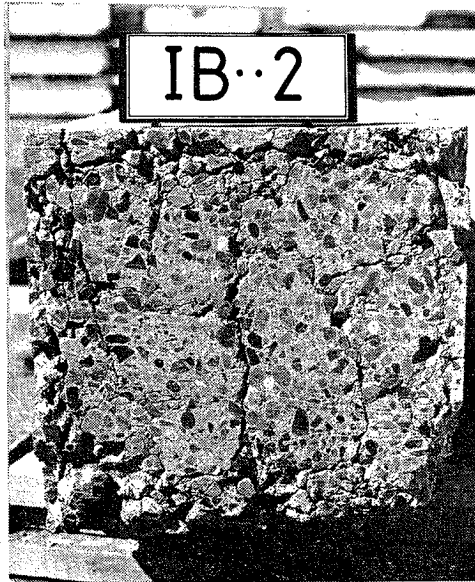


fig. 4

In order to study the phenomenon more closely, strain gauges were embedded in beam IB3. Fig. 5 shows a photograph of the embedded gauge in natural size.

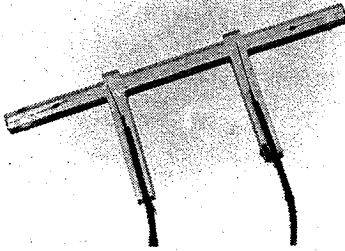


fig. 5

The measuring length is 17 mm and the gauge is enveloped in araldite.

The gauges were embedded with their measuring direction at right angles to one side face of the beam and so that their centrelines were located in the connecting line between the axial reinforcing bars on the side in question. Their positions are shown in fig. 6.

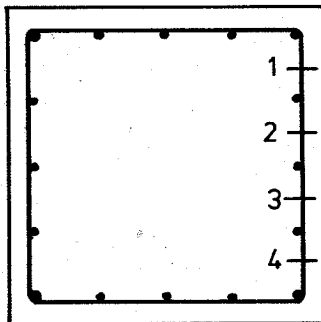


fig. 6.

Fig. 7 shows the measurements from gauges 1 and 2. Gauges 3 and 4 showed approximately the same picture.

The stress-strain curve for the beam in question is also shown in the figure. The same ordinate division is used, while the abscissa scale is a constant multiplied by the angle of torsion.

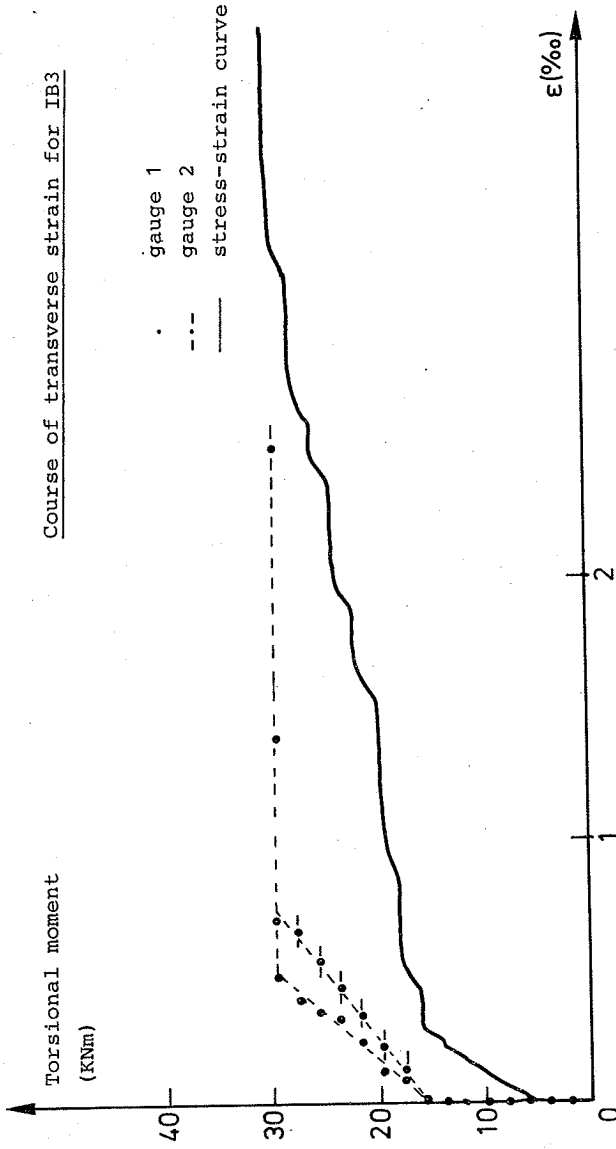


Fig. 7.

Until cracking occurred, the concrete was, as anticipated, free of stresses in the direction in question, while from commencement of cracking and up to rupture, there was an approximately linear relationship between the load increment and the strain. The ultimate strains achieved were bigger than is the case for pure tension, but as the stress field occurring here corresponded to the stress field for the case "concentrated line load", this is not surprising. The strains measured up to rupture are therefore interpreted as elastic deformation combined with transverse expansion on account of micro-cracking (as in ordinary compression testing). It has unfortunately not been possible to find tests with concentrated load applications, in which these deformations have been measured. The heavily increased strains at rupture (which resulted in the gauges being torn in two) show that the splitting crack shown in fig. 1 had now formed.

4. Theoretical treatment

In principle, the theory presented here is a lower-bound solution based on the theory of plasticity, two of the basic theorems of which are as follows:

The upper-bound theorem:

If the internal work for the displacement field belonging to a given mode of rupture that satisfies the geometrical boundary conditions is calculated, the load that gives the same external work will be greater than or equal to the ultimate carrying capacity.

Lower-bound theorem:

If it is possible to find a stress field which is in internal equilibrium throughout and which satisfies the statical and physical criteria, then the appurtenant load will be smaller than or equal to the ultimate carrying capacity.

4.1 Lower-bound solution

Let us consider a reinforced concrete beam subjected to pure torsion. The beam, which is shown in fig. 9, is assumed to be reinforced with hoops in the longitudinal direction and at right angles to this.

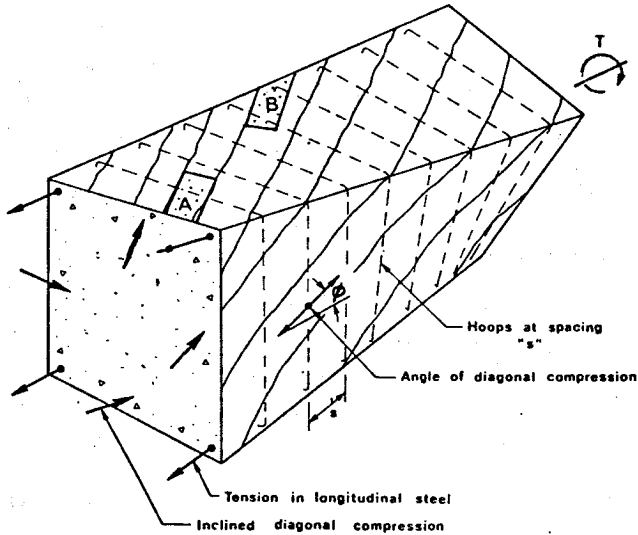


fig. 9.

We make the following assumptions:

- a) the concrete is in a plane state of stress and obeys the square yield criterion (fig. 10) with compressive yield strength σ_c and tensile yield strength 0.

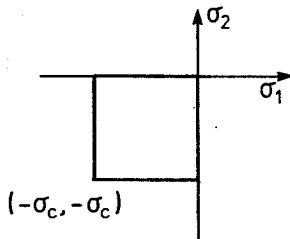


fig. 10.

- b) The reinforcing bars are perfectly plastic and are able to resist forces in their axial direction only.
- c) The action of the reinforcement in the direction of the beam axis can be described by an equivalent reinforcement force n_1 measured per unit length of the rectangle described by the corner bars. At yield $n_1 = n_{1y}$.
- d) The action of the reinforcement in the direction perpendicular to the beam axis can be described by an equivalent reinforcement force n_s measured per unit length of the beam axis. At yield, $n_s = n_{sy}$.

To obtain a lower bound for the torsional capacity, we assume the concrete between the corner bars to be in a state of homogenous, uniaxial compression inclined at the angle to the beam axis, with the resultant n_b measured per unit length in the perpendicular direction. At yield, $n_b = n_{by}$.

Moment equilibrium about the centre of the cross section requires (Bredt's formula):

$$T = \sqrt{2} a b n \quad (I)$$

where a = the biggest side length in the rectangle described by the corner bars.

b = the smallest side length in the rectangle described by the corner bars.

n = the shear force per unit length of the rectangle described by the corner bars.

We then consider the element as shown in fig. 11 (from fig. 9).

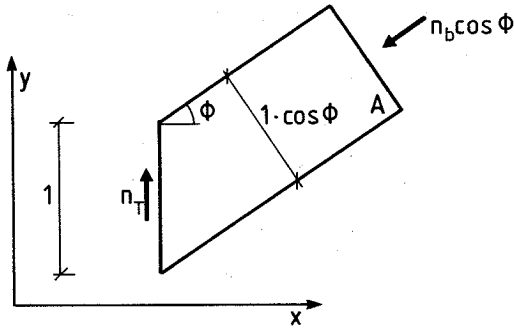


fig. 11.

Since equilibrium is required, we obtain:

$$n_x = -n_1 + n_b \times \cos^2 \phi$$

$$n = n_b \times \cos \phi \times \sin \phi$$

where $n_1; n_s$ = reinforcement forces per unit length

n_b = concrete force per unit length.

$n_x; n_y$ = normal forces per unit length

n = shear force per unit length.

Turning now to element B (from fig. 9), we obtain analogously from fig. 12:

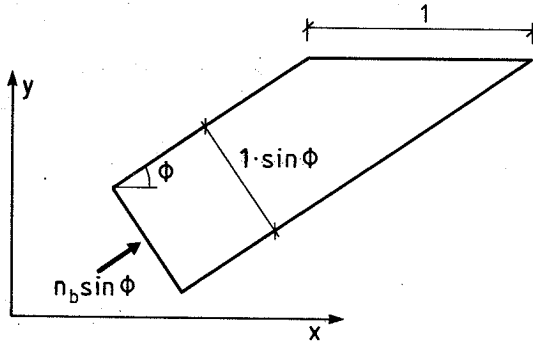


fig. 12.

$$n_y = -n_s + n_b \sin^2 \phi$$

Since n_x and n_y are equal to 0 (no normal force and for symmetry reasons), we obtain the following equations:

$$n_l = n_b \cdot \cos^2 \phi \quad (\text{II})$$

$$n_s = n_b \cdot \sin^2 \phi \quad (\text{III})$$

$$n_r = n_b \cdot \sin \phi \cdot \cos \phi \quad (\text{IV})$$

From II and III we obtain:

$$\text{tg} \phi = \sqrt{\frac{n_s}{n_l}} \quad (\text{V})$$

$$n_b = n_s + n_l \quad (\text{VI})$$

and from I, II, III and IV, we obtain

$$T = 2ab \cdot \sqrt{n_l \cdot n_s}$$

As T is an increasing function of n_1 and n_s , we obtain the biggest lower bound for

$$n_1 = n_{ly} \quad \text{and} \quad n_s = n_{sy};$$

$$T = 2ab \cdot \sqrt{n_{ly} \cdot n_{sy}}$$

with the angle \emptyset determined by

$$\text{tg}\emptyset = \sqrt{\frac{n_{sy}}{n_{ly}}}$$

This equation is valid as long as the force per unit length n_b does not exceed the yield force n_{by} , in other words,

$$n_{ly} + n_{sy} \leq n_{by}$$

For $n_{ly} + n_{sy} > n_{by}$

there are three possibilities:

1) for $(n_{sy} \leq \frac{1}{2}n_{by}) \wedge (n_1 = n_{by} - n_{sy} < n_{ly})$,

i.e., the reinforcement in the longitudinal direction does not yield, we get:

$$T = 2ab\sqrt{n_{sy}(n_{by} - n_{sy})} \quad (B)$$

with the angle \emptyset determined by

$$\text{tg}\emptyset = \sqrt{\frac{n_{sy}}{n_{by} - n_{sy}}}$$

2) for $(n_{ly} \leq \frac{1}{2}n_{by}) \wedge (n_s = n_{by} - n_{ly} < n_{sy})$,

i.e., the reinforcement in the direction of the stirrups does not yield, we get:

$$T = 2ab\sqrt{n_{ly}(n_{by} - n_{ly})} \quad (C)$$

with the angle ϕ determined by

$$\operatorname{tg}\phi = \sqrt{\frac{n_{by} - n_{ly}}{n_{ly}}}$$

- 3) for $(n_{ly} \geq \frac{1}{2}n_{by}) \wedge (n_{sy} \geq \frac{1}{2}n_{by})$,

we obtain the biggest lower bound for $n_l = n_s = \frac{1}{2} n_{by}$,
i.e. yielding is not reached in either the axial
direction or the stirrup direction:

$$T = 2ab \sqrt{\frac{1}{2}n_{by} \cdot \frac{1}{2}n_{by}} \Rightarrow$$

$$T = ab \cdot n_{by} \tag{D}$$

with the angle ϕ determined by

$$\operatorname{tg}\phi = \sqrt{\frac{\frac{1}{2}n_{by}}{\frac{1}{2}n_{by}}} = 1$$

The system of equations A - D represents a complete system of equations for solving the torsional carrying capacity for all degrees of reinforcement. In addition to n_{sy} and n_{ly} , the determination of which presents no problems, the unknown quantities include the quantity n_{by} , which we attempt to determine in the last part of this section.

4.2 Determination of n_{by}

It can be concluded from the test observations that n_{by} is independent of the thickness of the concrete cover, but that it depends on the arrangement of the reinforcement used - and especially the diameter of the axial reinforcing bar located at the corner of the cross section.

The tests also showed that the strength parameters of the concrete must also be included in the expression for n_{by} , and we can therefore expect an expression of the form :

$$n_{by} = f(d; \sigma_c; \sigma_t; \dots\dots)$$

where:

d = the diameter of the longitudinal reinforcing bar located at the corner of the cross section.

σ_c = the compression strength of the concrete.

σ_t = the tensile strength of the concrete

In order to create equilibrium in a corner element, the compression in the concrete n_b must be transmitted to the reinforcement, and if this force transmission is assumed to take place uniformly along the axial reinforcing bars located at the corner, we can draw analogies to the subject:

"concentrated line loads on concrete bodies."

Within this field, there are many studies and empirical expressions, but when applied to this special area, those commonly used do not give expressions with acceptable functional correlation - and do not give reasonable numerical values either.

For calculating the quantity n_{by} , use is therefore made of an upper bound solution from the theory of plasticity for the case: concentrated line load on unreinforced concrete prisms.

The rupture patterns and calculation of the upper bound for this case have been published by W.F. Chen and D.C. Drucker [5].

Here, too, an attempt has been made to establish a safe, statically admissible stress field (lower bound solution) on the same assumptions as used for the upper bound solution. The efforts were not crowned with success, and we must therefore make do with the upper bound.

In a lower bound solution (here the solution of the determination of the torsional strength of the beam) it may be dangerous to incorporate strength parameters determined on the basis of upper bound solutions for sub-problems since one is then no longer sure that one's result is going to be on the safe side of the actual ultimate load, even when the assumptions are satisfied. However, the rupture pattern used for determination of n_{by} is in accordance with the observed pattern, and the upper bound solution can also be expected to be close to the right solution. For this reason we will continue to regard the expression for determination of the torsional moment of the beam as a true lower bound.

4.2.1 Plastic determination of n_{by}

The following assumptions are made:

- a) It is assumed that there is a plane deformation field.
- b) The concrete is regarded as a stiff, plastic material, the yield criterion of which follows Coulomb's modified rupture hypothesis.
- c) Rupture is assumed to take the form of split rupture with the rupture pattern shown in fig. 13.

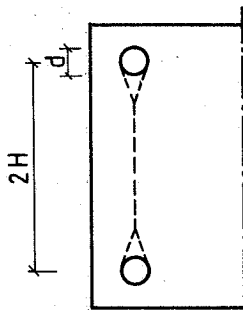


fig. 13

- d) The rupture value corresponding to the rupture pattern shown in fig. 13 is assumed to be the same as for the rupture pattern in fig. 14.

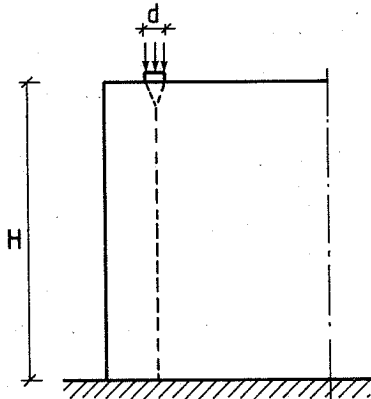


fig. 14.

re b) The actual material properties of the concrete lie far from those assumed here - especially as regards the concrete's tensile properties. This is a trivial problem in all applications of the theory of plasticity to concrete, and here (as, for example, in [6] or [8]), we compensate for these deficiencies by assuming that both the tensile strength and the compression strength are a product of an effectivity factor and the measured material strength.

The size of these effectivity factors is determined (for lack of a better method) on the basis of the test results.

It is obvious, in advance, that both these factors must lie between zero and unity, and it must be assumed that the effectivity factor for compression v_c is considerably bigger than that for tension v_t . If we assume $v_t = 0$, we get the stress in the loading face $\leq \sigma_c$, which is clearly at variance with tests with concentrated loads. We must therefore assume that $0 < v_t < v_c \leq 1$.

However, the expressions in the following have been derived on the assumption that the measured uniaxial values can be used for the tensile strength and the compression strength, and the effectivity factors are first introduced in the section on comparison with tests.

re c) Only this rupture pattern is investigated since it is in accordance with the observed pattern. This is warranted because other possible rupture patterns with a rupture load are not applicable owing, for example, to bigger appurtenant effectivity factors.

The assumed rupture pattern presupposes a horizontal displacement of the loading face in relation to the two parts of the concrete. Such displacement can easily be established on the section between two hoops. At one hoop, the matter becomes more problematical, and (even though the practical design of a corner detail helps us, see fig. 15) we probably have to assume that the rupture pattern is locally as indicated in fig. 16.

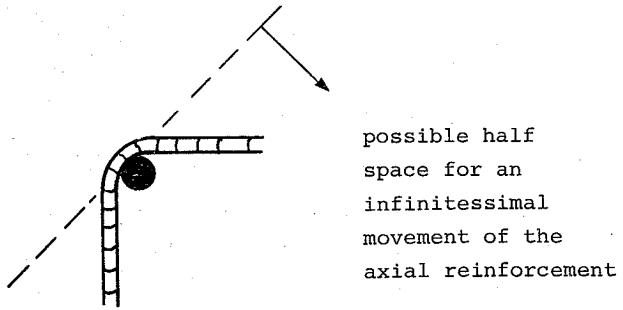


fig. 15

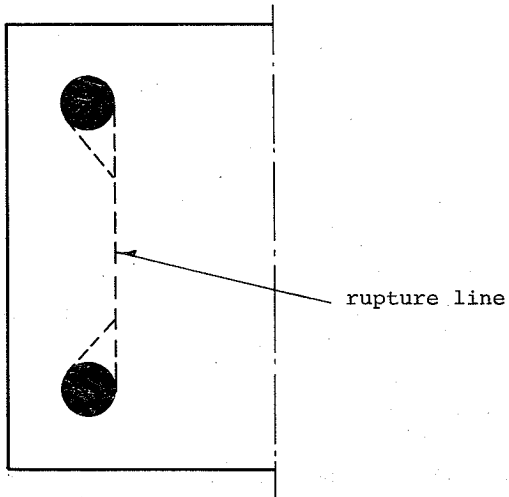


fig. 16

As this rupture pattern is difficult to handle purely arithmetically and as it must be assumed only to occur locally, we have chosen to regard the rupture pattern shown in fig. 14 as valid throughout.

4.2.1.1 Description of rupture pattern

The wedge that is formed directly under the concentrated load moves downwards, and the remaining two parts of the prism move out to the sides. We thereby get sliding failure along the sides of the wedge and separation failure along the vertical split. If we assume that the apex of the wedge is $2 \cdot \beta$ and that the relevant movement V along the sides of the wedge form the angle φ (= the angle of friction) with this, we get the relationship shown in fig. 17 between the movements.

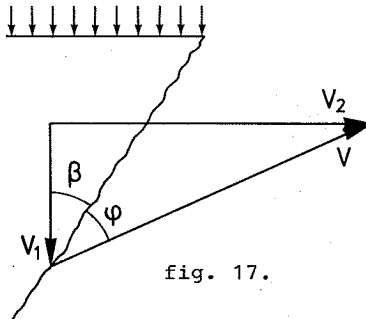


fig. 17.

In this figure, V_1 is the vertical movement of the wedge, and $2 \cdot V_2$ is the total horizontal movement in the vertical discontinuity line. By means of the assumed yield surface for the concrete and the displacement field sketched here, we can calculate both the internal and the external work required for the displacement, and the resulting value of the concentrated pressure is minimized with regard to the angle β (for further explanation, see [5]).

External work:

$$A_y = \sigma_f \cdot d \cdot V \cdot \cos(\beta + \varphi)$$

Internal work:

$$A_i = \sigma_t \left(H - \frac{d}{2} \cot \beta \right) \cdot 2 \cdot V \cdot \sin(\beta + \varphi) + \frac{1 - \sin \varphi}{2} \cdot \sigma_c \cdot \frac{d}{\sin \beta} \cdot V$$

From $A_y = A_i$, we get

$$\sigma_f = \frac{\frac{1}{2}(1 - \sin \varphi) \sigma_c + \sin(\beta + \varphi) \left(\frac{2H}{d} \sin \beta - \cos \beta \right) \sigma_t}{\sin \beta \cos(\beta + \varphi)}$$

which has its minimum value for:

$$\cot \beta = \operatorname{tg} \varphi + \frac{1}{\cos \varphi} \sqrt{1 + \frac{(2H/d) \cos \varphi}{(\sigma_c / \sigma_t) \left(\frac{1 - \sin \varphi}{2} - \sin \varphi \right)}}$$

Inserted in the expression for σ_f , this gives:

$$\sigma_f = \sigma_t \left(\frac{2H}{d} \operatorname{tg}(2\beta + \varphi) - 1 \right)$$

The quantity H is determined here as shown in fig. 18.

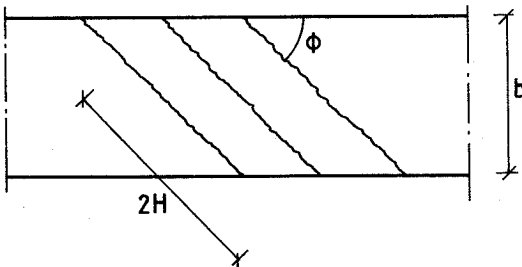


fig. 18.

$$b = 2H \sin \varphi \Rightarrow$$

$$H = \frac{b}{2} \frac{1}{\sin \varphi}$$

which, inserted in the expression for $d \cdot \sigma_f$, gives:

$$n_{by} = d \cdot \sigma_t \left(\frac{b}{d} \frac{\operatorname{tg}(2\beta + \varphi)}{\sin \varphi} - 1 \right)$$

where

b = smallest side length in the rectangle described by the axial reinforcement

d = the diameter of an axial reinforcing bar at a corner of a cross section

\emptyset = the angle between the longitudinal axis of the beam and the direction of the compression in the concrete

φ = the angle of friction of the concrete = 37°

β : determined from the following expression:

$$\cot \beta = \operatorname{tg} \varphi + \frac{1}{\cos \varphi} \sqrt{1 + \frac{\frac{b}{d} \frac{\cos \varphi}{\sin \varphi}}{\frac{\sigma_c}{\sigma_t} \left(\frac{1 - \sin \varphi}{2} - \sin \varphi \right)}}$$

where:

σ_c = the cylinder compression strength of the concrete

σ_t = the split tensile strength of the concrete.

5. Comparison with tests

As in every other application of the theory of plasticity to concrete structures, the analysis is only useful if it produces a result that is in reasonable accordance with the experimental results, and the theory from the foregoing pages will therefore now be compared with test results.

Two test series have been chosen for the comparison: one performed by John Sander Nielsen and Troels Brøndum Nielsen (mentioned in section 3 and described in greater detail in [3]) and one performed by Paul Lampert and Bruno Thürliman at Institut für Bau- statik ETH Zürich [7]. The main data from the former series are given in tables 1, 2 and 3, and the main data from the latter in table 4.

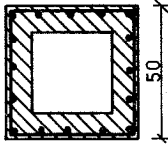
Beam	Cross section cm	Longitudinal reinforcement	Stirrup reinforcement	$\sigma_{F\&}$ kg/cm ²	σ_{fb} kg/cm ²	σ_c kg/cm ²	Measured carrying capacity V_0 tm	Calculated carrying capacity V_0 tm
T ₀		16 ϕ 16	ϕ 16 pr. cm	3520	3520	320	21.1	25.8

TABLE 4.

The beams in which yielding of the reinforcement was not ascertained were used for determining the efficiency factors mentioned on page 54. The determination was performed on a computer by calculating n_{by} for all combinations of v_t and v_c , and comparing the results with n_b .

Assuming the concrete compression force (per unit of length) corresponding to the observed ultimate strength to be an expression of a normally distributed function with a specific mean value and standard deviation, where the mean value is a function of v_c and v_t , $f(v_c, v_t)$, we obtain (by means of the maximum likelihood principle) the best determination of v_c and v_t by minimizing the expression

$$\sum_{i=1}^n (n_{bi} - f_i(v_t, v_c))^2 = Q(v_t, v_c)$$

where n = the number of tests

$$f(v_t, v_c) = d \cdot \sigma_f(v_t, v_c)$$

Owing partly to the limited number of test beams, the efficiency factors have only been determined to one decimal point, and the factors given below must therefore be regarded only as a guide:

$$v_c = 0.6$$

$$v_t = 0.3$$

Inserting these values for the efficiency factors in the expressions for σ_f , we obtain the following anticipated values of n_{by} compared with the observed values:

Beam No.	n_{by} , tests MPa	n_{by} , theory MPa
IB2	4,77	4,58
IB3	4,84	4,64
II 0	5,55	5,53
II 1	5,57	5,76
II 2	6,27	6,27
II 4*	5,66	5,51
II 5*	6,09	5,92
II 6*	5,98	6,40
II 8	5,26	5,34
T ₀	11,41	11,57

TABLE 5

As a measure of the degree of over-reinforcement, we use here the quantity:

$$\frac{n_{xa} + n_{ya}}{n_{by}}$$

Fig. 19 shows $\frac{V_{exp}}{V_{theory}}$ as a function of this parameter, where

$\frac{n_{xa} + n_{ya}}{n_{by}} = 1$ gives the upper bound for normally reinforced cross sections.

φ is put at 37° .

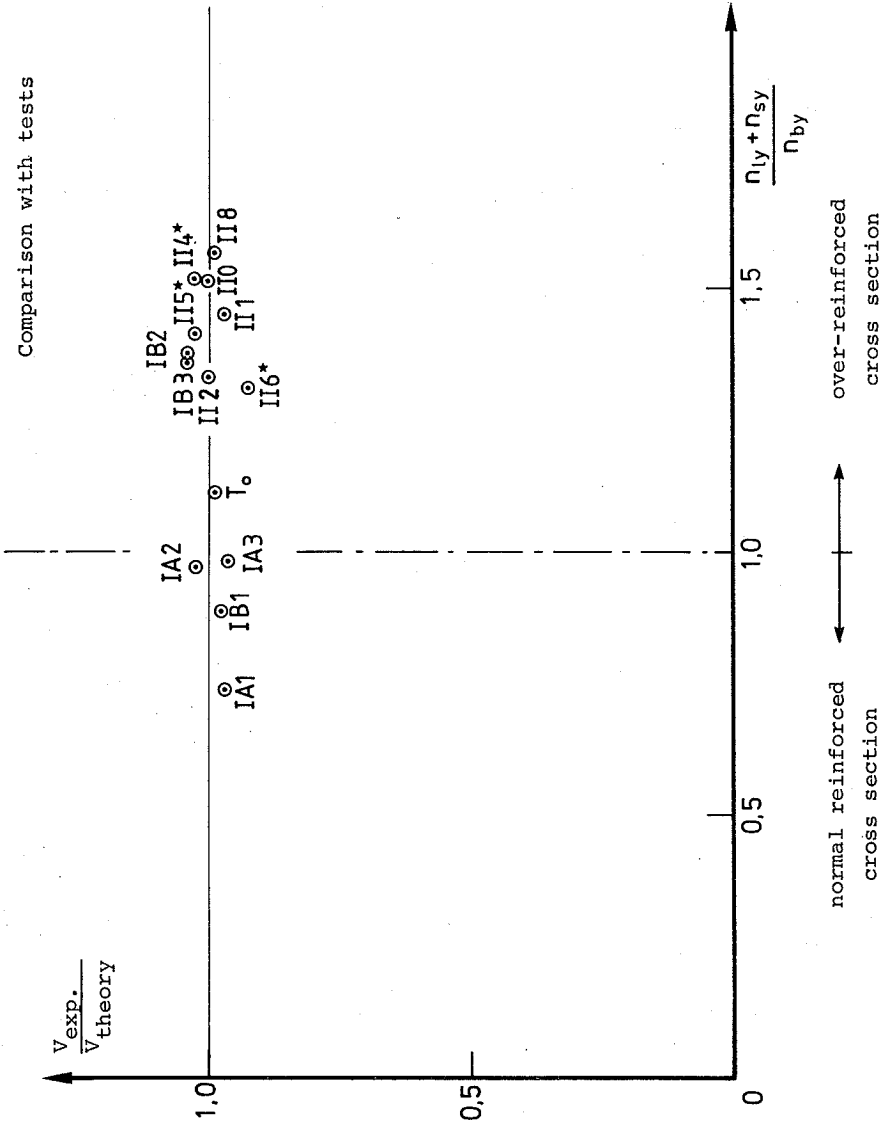


fig. 19.

6. Conclusions and discussion

Accordance between the calculated and the observed values of the ultimate strength must be said to be satisfactory, and the numerical values of the efficiency factors lie within the anticipated interval. As the comparative material represents a reasonable interval for the parameters taken into account (σ_c , σ_t , b , d), the system of equations on page 24 to 27, combined with the determination of n_{by} on page 33, must be said to constitute a complete system for analysing the torsional carrying capacity of reinforced concrete beams.

A variation of the angle \emptyset would have been desirable, but it was impossible to find test results that satisfactorily illuminated the effect of this quantity.

Two questions now arise:

- 1: the accordance between the presented here and that proposed in DS411 [9].
- 2: the combination of a torsional and a bending moment.

re 1) If we introduce the following in the expression for n_{by} (from page 33)

$$v_c = 0.6$$

$$v_t = 0.3$$

$$\emptyset = 45^\circ$$

$$\sigma_t = \frac{1}{10} \sigma_c$$

and convert n_{by} into an equivalent stress in a hollow cross section with the wall thickness $t = \frac{b}{5}$ (as described in DS411), we obtain, by assuming $d = \frac{1}{24} b$

$$\sigma_{b(\max)} = 0.4 \sigma_c$$

and we thus see that there is complete accordance for the assumptions made here.

All the assumptions made (apart from $d = \frac{1}{24} b$) appear reasonable. The assumption that $d = \frac{1}{24} b$ is also in reasonable accordance with the basic test material for the code, although it seems to be unreasonable in the case of big structures. It must therefore be presumed that the directions given in the code will result in structures whose carrying capacity is on the unsafe side unless it is ensured that the longitudinal reinforcement at the corner of the cross section satisfies the criterion $d \geq \frac{1}{24} b$, or the reinforcement is arranged in such a way as to give an equally good possibility of force transmission.

re 2) Here, only the case in which it is the concrete that sets an upper bound for the carrying capacity will be considered. This case is of great practical importance to designers on account of the interaction between the compression stresses in the concrete from bending and torsion.

We will therefore try to find a reasonable interaction diagram for the concrete compression stresses produced by these two forces.

DS411 (guide) proposes the diagram shown in fig. 20, while "CEB Model Code" [10] mainly recommends the diagram shown by the broken line in fig. 20.

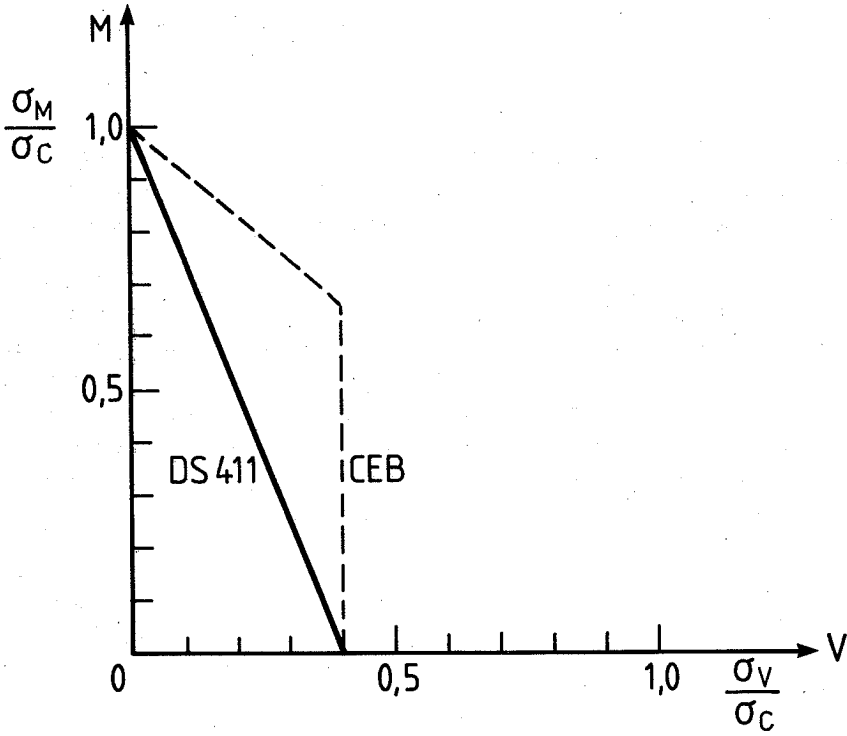


fig. 20.

Whereas DS411 must be presumed to be too conservative, it seems unreasonable, in the CEB Model Code, to allow loading with a bending moment as shown by the vertical line for $= 0.4 \cdot \sigma_c$, even when the concrete has been fully utilized for torsion.

The theory for the treatment of pure torsion will therefore be extended here in order to construct an interaction diagram for the compression stresses in the compression zone of the concrete (from bending).

We assume the same mode of rupture and must therefore be able to use the expression for n_{by} . The expressions for determination of \emptyset no longer apply, however, although this can still be determined as the angle between the longitudinal axis of the beam and the direction of the resultant of the compression in the concrete (in the compression zone). With similar assumptions as in point 1, viz.

$$v_c = 0.6$$

$$v_t = 0.3$$

$$\sigma_t = \frac{1}{10} \sigma_c$$

$$d = \frac{1}{24}$$

and converting n_{by} into an equivalent stress in a hollow cross section with the wall thickness $t = \frac{1}{5} \cdot b$, we obtain the following formula by insertion in the equations on pages 33 and 34:

$$I: n_{by} = \sigma_{by} \cdot d \cdot \frac{1}{10} \cdot 0.3 \cdot \sigma_c \left(\frac{b}{d} \frac{\operatorname{tg}(2\beta + 37^\circ)}{\sin \emptyset} - 1 \right)$$

where β is determined by

$$II: \cot \beta = \operatorname{tg} 37^\circ + \frac{1}{\cos 37^\circ} \cdot$$

$$\cdot \sqrt{1 + \frac{24 \frac{\cos 37^\circ}{\sin \emptyset}}{0.6 \cdot \sigma_c} \cdot \frac{1}{0.3 \cdot \frac{1}{10} \cdot \sigma_c} (1 - \sin 37^\circ - \sin 37^\circ)}$$

Putting σ_{by} equal to a code factor (f_n) multiplied by σ_c , we obtain, by insertion and calculation of I and II:

$$\text{I: } f_n \cdot \sigma_c \cdot \frac{1}{5}b = d \cdot \frac{1}{10} \cdot 0.3 \cdot \sigma_c \cdot \left(\frac{b}{d} \frac{(\operatorname{tg} 2\beta + 37^\circ)}{\sin\emptyset} - 1 \right)$$

$$f_n = 0.15 \cdot \left[\frac{\operatorname{tg}(2\beta + 37^\circ)}{\sin\emptyset} - \frac{1}{24} \right]$$

$$\text{II: } \cot\beta = 0.75 + 1.25 \cdot \sqrt{1 + \frac{5.67}{\sin\emptyset}}$$

The total interaction diagram is obtained by plotting f_n vectorially, in a V-M diagram with axes at 45° , as the length of a vector with the slope $\frac{M}{V}$.

The angle \emptyset is determined as the angle of the compression resultant (in the compression flange) with the axis of the beam. We then let \emptyset run through the interval from 0 to 45° and obtain the desired curve by insertion in I and II and by using the self-evident criterion that the compression resultant is always smaller than σ_c . Dissolved in a normal M-V diagram, we obtain the following curve and table:

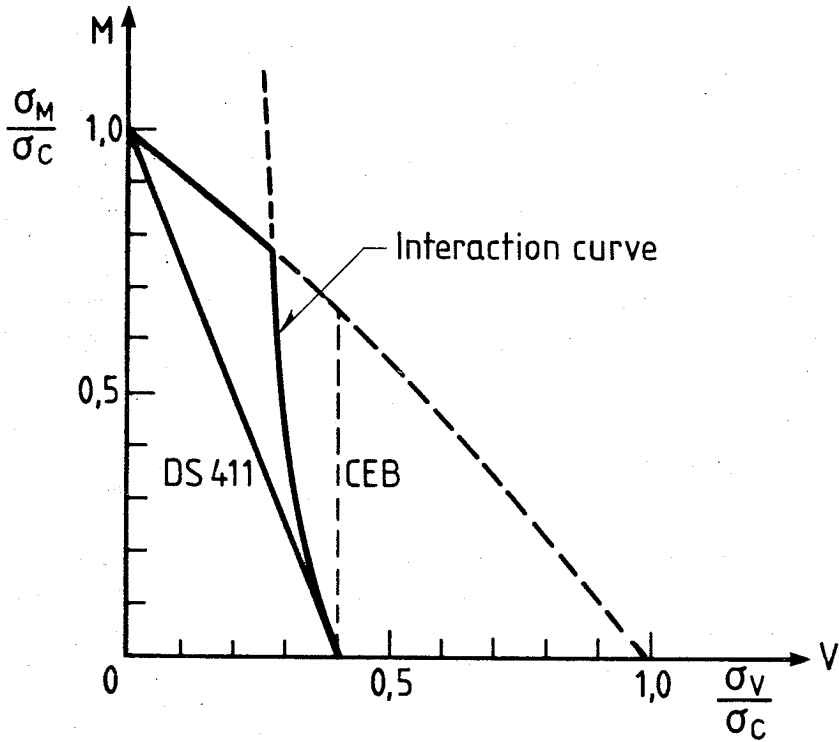


fig. 21.

\emptyset	β	f_n	$f_n \cdot \frac{\sigma_V}{\sigma_C}$	$f_n \cdot \frac{\sigma_M}{\sigma_C}$
45	12.51	0.393	0.393	0
40	12.09	0.418	0.380	0.051
35	11.59	0.450	0.365	0.111
30	11.01	0.493	0.349	0.181
25	10.63	0.567	0.339	0.275
20	9.48	0.643	0.311	0.384
15	8.45	0.788	0.289	0.557
10	8.00	1.140	0.280	0.925
5	5.24	1.870	0.230	1.700
$\rightarrow 0$	$\rightarrow 0$	$\rightarrow \infty$	$\rightarrow 0$	$\rightarrow \infty$

TABLE 5.

An acceptable approximation to the curve in fig. 21 can be obtained by a bilinear relationship. This has been suggested to the Danish Concrete Code Committee for incorporation in the revised edition of the Danish Code for Concrete Structures.

REFERENCES

- 1 : Lennart Elfgren and Inge Karlson,
Vridning av betongkonstruktioner. Betongbyggnad
rapport 69:2, 1969. Chalmers Tekniska Högskola.
- 2 : Denis Mitchell and Michael P. Collins,
The behaviour of Structural Concrete in pure Torsion,
Publication 74-06, University of Toronto.
- 3 : John Sander Nielsen,
A Theoretical and Experimental Study of Concrete Beams -
Especially Over-Reinforced Beams - Subjected to Torsion.
Part II Experiments.
- 4 : John Sander Nielsen,
The effect of stirrup spacing on the ultimate load
of reinforced concrete beams subjected to pure torsion.
- 5 : W.F. Chen and D.C. Drücker,
Bearing capacity of concrete blocks or rock,
Journal of the Eng.Mech.Div. ASCE vol. 95 No. EM4 1969.
- 6 : M.W. Bræstrup,
Shear tests on reinforced concrete T-beams,
Rapport nr. R72, 1976. ABK, DTH.
- 7 : Lampert und Thürlimann,
Torsionsversuche and Stahlbetonbalken,
Bericht Nr. 6506-2, Institut für Baustatik, ETH,
Zürich, Juni 1968.

AFDELINGEN FOR BÆRENDE KONSTRUKTIONER

DANMARKS TEKNISKE HØJSKOLE

Department of Structural Engineering
 Technical University of Denmark, DK-2800 Lyngby

SERIE R

(Tidligere: Rapporter)

- R 126. GIMSING, NIELS J.: Four Papers on Cable Supported Bridges. 1980.
- R 127. SVENSSON, SVEN EILIF og JAN KRAGERUP: Interaktiv bæreevne af sammensatte søjler. 1980.
- R 128. GIMSING, NIELS J. og JØRGEN GIMSING: Analysis of Erection Procedure for Bridges with Combined Cable Systems. Cable Net Bridge Concept. 1980.
- R 129. ROSTAM, STEEN og EIGIL STEEN PEDERSEN: Partially Prestressed Concrete Bridges. Danish Experience. 1980.
- R 130. BRØNDUM-NIELSEN, TROELS: Stress Analysis of Cracked Arbitrary Concrete Section under Service Load. 1981.
- R 131. BRINCKER, RUNE: Plane revneudvidelsesproblemer i lineært viscoelastiske materialer. Løsning af plane lineært viscoelastiske randværdiproblemer med kendt revneudbredelsesforløb. 1982.
- R 132. BRINCKER, RUNE: Plane revneudbredelsesproblemer i lineært viscoelastiske materialer. Revnemodeller og udbredelseskrifter. 1983.
- R 133. Reserveret.
- R 134. ABK's informationsdag 1981. 1981.
- R 135. Resumeoversigt 1980. Summaries of Papers 1980. 1981.
- R 136. BACH, FINN og M.P. NIELSEN: Nedreværdiløsninger for jernbetonplader. 1981.
- R 137. Publication pending.
- R 138. NIELSEN, LEIF OTTO og PETER NITTEGAARD-NIELSEN: Elementmetodeberegninger på mikrodatamat. 1981.
- R 139. MONDORF, P.E.: Concrete Bridges. Literature Index. 1981.
- R 140. NIELSEN, METTE THIEL: Lamb's Problem. Internal Harmonic Point Load in a Half-Space. 1981.
- R 141. JENSEN, JESPER FRØBERT: Plasticitetsteoretiske løsninger for skiver og bjælker af jernbeton. 1982.
- R 142. MØLLMANN, H.: Thin-Walled Elastic Beams with Finite Displacements. 1981.
- R 143. KRAGERUP, JAN: Five Notes on Plate Buckling. 1982.
- R 144. NIELSEN, LEIF OTTO: Konstitutiv modellering af friktionsdæmpning. 1982.
- R 145. NIELSEN, LEIF OTTO: Materiale med friktion til numeriske beregninger. 1982.
- R 146. Resumeoversigt 1981. Summary of Papers 1981. 1982.
- R 147. AGERSKOV, H. and J. BJØRNBÆK-HANSEN: Bolted End Plate Connections in Round Bar Steel Structures. 1982.
- R 148. NIELSEN, LEIF OTTO: Svingninger med friktionsdæmpning. 1982.
- R 149. PEDERSEN, CARL: Stability Properties and Non-Linear Behaviour of Thin-Walled Elastic Beams of Open Cross-Section. Part 1: Basic Analysis. 1982.
- R 150. PEDERSEN, CARL: Stability Properties and Non-Linear Behaviour of Thin-Walled Elastic Beams of Open Cross-Section. Part 2: Numerical Examples. 1982.

- R 151. KRENCHER, HERBERT and HANS WINDBERG JENSEN: Organic Reinforcing Fibres for Cement and Concrete. 1982.
- R 152. THIEL, METTE: Dynamic Interaction between Soil and Foundation. 1982.
- R 153. THIEL, METTE: Soil-Pile Interaction in Horizontal Vibration. 1982.
- R 154. RIBERHOLT, H. og PER GOLTERMANN: Sømmede træbjælker. 1982.
- R 155. JENSEN, JENS HENNING: Forkammede armeringsstængers forankring, specielt ved vederlag. 1. del. 1982.
- R 156. JENSEN, JENS HENNING: Forkammede armeringsstængers forankring, specielt ved vederlag. 2. del. Appendix A til F. 1982.
- R 157. ARPE, ROBERT and CLAES DYRBYE: Elasto-Plastic Response to Stochastic Earthquakes. 1983.
- R 158. WALD, FRANTISEK: Non-Linear Analysis of Steel Frames (with Special Consideration of Deflection). 1983.
- R 159. BRÆSTRUP, MIKAEL W.: Ten Lectures on Concrete Plasticity. Course given in Nanjing, China, October 1982. 1983.
- R 160. FEDDERSEN, BENT og M.P. NIELSEN: Opbøjet spændarmering som forskydningsarmering. 1983.
- R 161. KRAGERUP, JAN: Buckling of Rectangular Unstiffened Steel Plates in Compression. 1983.
- R 162. FEDDERSEN, BENT og M.P. NIELSEN: Revneteorier for enaksede spændingstilstande. 1983.
- R 163. Reserveret.
- R 164. GIMSING, NIELS J.: Preliminary Design and Optimization of Cable Systems for Bridges. 1983.
- R 165. Resuméoversigt 1982. Summaries of Papers 1982. 1983.
- R 166. NITTEGAARD-NIELSEN, PETER, JOHN FORBES OLESEN og HILMER RIBERHOLT: Elementmetodeberegning af skiveafstivede lamelkonstruktioner. 1983.
- R 167. RIBERHOLT, HILMER og PETER SPØER: Indlimede bolte til indfæstning af vingerne på Nibemølle-B. 1983.
- R 168. GIMSING, NIELS J. and ANDERS BORREGAARD SØRENSEN: Investigations into the Possibilities of Constructing Bridges with a Free Span of 3000 m. 1983.